nature geoscience

LETTERS

PUBLISHED ONLINE: 14 APRIL 2013 | DOI: 10.1038/NGEO1779

Photochemical production of molecular bromine in Arctic surface snowpacks

Kerri A. Pratt[1]*, Kyle D. Custard[1], Paul B. Shepson[1,2], Thomas A. Douglas[3], Denis Pöhler[4], Stephan General[4], Johannes Zielcke[4], William R. Simpson[5], Ulrich Platt[4], David J. Tanner[6], L. Gregory Huey[6], Mark Carlsen[1] and Brian H. Stirm[7]

Following the springtime polar sunrise, ozone concentrations in the lower troposphere episodically decline to near-zero levels[1]. These ozone depletion events are initiated by an increase in reactive bromine levels in the atmosphere[2–5]. Under these conditions, the oxidative capacity of the Arctic troposphere is altered, leading to the removal of numerous transported trace gas pollutants, including mercury[6]. However, the sources and mechanisms leading to increased atmospheric reactive bromine levels have remained uncertain, limiting simulations of Arctic atmospheric chemistry with the rapidly transforming sea-ice landscape[7,8]. Here, we examine the potential for molecular bromine production in various samples of saline snow and sea ice, in the presence and absence of sunlight and ozone, in an outdoor snow chamber in Alaska. Molecular bromine was detected only on exposure of surface snow (collected above tundra and first-year sea ice) to sunlight. This suggests that the oxidation of bromide is facilitated by a photochemical mechanism, which was most efficient for more acidic samples characterized by enhanced bromide to chloride ratios. Molecular bromine concentrations increased significantly when the snow was exposed to ozone, consistent with an interstitial air amplification mechanism. Aircraft-based observations confirm that bromine oxide levels were enhanced near the snow surface. We suggest that the photochemical production of molecular bromine in surface snow serves as a major source of reactive bromine, which leads to the episodic depletion of tropospheric ozone in the Arctic springtime.

Proposed substrates for Arctic halogen activation include open water, frost flowers, sea ice, surface snow, blowing snow and aerosols[7]. To test the effectiveness of various snow and ice surfaces for bromine activation, ten outdoor snow chamber experiments were conducted during the March–April 2012 Bromine, Ozone and Mercury Experiment (BROMEX) in Barrow, Alaska. As listed in Table 1, locally obtained samples included first-year sea ice, brine icicles that drained through the base of uplifted sea-ice blocks, several different layers of snow located on first-year sea ice, and surface snow on the tundra. Real-time chemical ionization mass spectrometry was used to monitor Br_2 production[9] from the snow/ice samples in a perfluoroalkoxy-coated chamber, through which clean air, with and without ozone, was allowed to flow. Br_2 was observed only when snow samples were exposed to ambient sunlight, as shown in Fig. 1 and in the Supplementary Information. This indicates active snowpack photochemistry. On O_3 addition, chamber Br_2 concentrations increased, consistent with the autocatalytic bromine explosion mechanism, described below.

Photochemical production of the hydroxyl radical (OH) in the snowpack condensed phase and the subsequent oxidation of bromide explains the initially observed Br_2 production. Photoactivated release of Br_2 into the atmosphere was previously proposed to explain boundary-layer ozone destruction beginning at polar sunrise[2]. In our experiments, ~3 ppt of Br_2 was produced from naturally sunlit tundra surface snow with O_3-free air flow (Fig. 1b and Supplementary Fig. S9). This is consistent with laboratory-based observations of Br_2 production from condensed-phase OH formation and subsequent reaction with bromide within the surface liquid layer of frozen solutions of chloride, bromide, iodide and nitrate[10]. Condensed-phase photolysis of H_2O_2 and nitrite (NO_2^-) has been shown to produce ~96% of the OH in the Barrow snowpack, with nitrate (NO_3^-) suggested to be an important precursor elsewhere[11]. Although H_2O_2 photolysis produces OH leading to Br_2 formation, H_2O_2 also reacts with Br_2 and can inhibit Br_2 release[12]. For our chamber experiments, the suggested initialization mechanism of Br_2 release to the interstitial snowpack air is shown in Fig. 2, wherein nitrite and H_2O_2 photolysis lead to condensed-phase OH production and reaction with bromide under acidic conditions within the quasi-brine layer that forms at the snow grain surface[10,13].

The most efficient Br_2 production was observed for tundra snow and the top 1 cm of surface snow above first-year sea ice. These samples were characterized by lower salinity, lower pH (4.6–6.3) and higher Br^-/Cl^- molar ratios (1/148–1/38) compared with the snow and ice samples (sea ice, brine icicles and basal snow directly above sea ice) that did not exhibit Br_2 production (bromide/chloride ratios of 1/526–1/230, pH 7.3–9.5; Table 1). The basal snow, collected from the sea-ice surface to 8 cm directly above first-year sea ice, was impacted by the upward migration of brine[14]. In contrast, the top layer of surface snow above the first-year sea ice was impacted by atmospheric aerosol and trace gas deposition, which led to the observed higher Br^-/Cl^- ratios[14] and lower pH. The

[1]Department of Chemistry, Purdue University, West Lafayette, Indiana 47907, USA, [2]Department of Earth, Atmospheric, and Planetary Sciences and Purdue Climate Change Research Center, Purdue University, West Lafayette, Indiana 47907, USA, [3]US Army Cold Regions Research and Engineering Laboratory, Fort Wainwright, Alaska 99703, USA, [4]Institute of Environmental Physics, University of Heidelberg, D-69117 Heidelberg, Germany, [5]Geophysical Institute and Department of Chemistry, University of Alaska Fairbanks, Fairbanks, Alaska 99775, USA, [6]School of Earth and Atmospheric Sciences, Georgia Institute of Technology, Atlanta, Georgia 30332, USA, [7]Department of Aviation Technology, Purdue University, West Lafayette, Indiana 47907, USA. *e-mail: kapratt@purdue.edu.

Table 1 | Snow and ice compositions corresponding to the ten chamber experiments.

Experiment date	Sample type	pH	Br^- (μM)	Br^-/Cl^-	Br_2 observed?
14 March 2012	Sea ice	7.3	161 (13)	1/526 (1/158)	No
13 March 2012	Brine icicles	9.5	677 (48)	1/230 (1/18)	No
16 March 2012	Basal snow (0–8 cm) above sea ice	7.5	61 (6)	1/434 (1/49)	No
21 March 2012	Sintered snow (8–18 cm) above sea ice	5.3	2.19 (0.09)	1/468 (1/177)	*
26 March 2012	Surface snow (top 1 cm) above sea ice	5.6	11.4 (0.6)	1/99 (1/22)	Yes
8 March 2012	Tundra surface snow	4.8	0.16 (0.02)	1/148 (1/24)	Yes
19 March 2012	Tundra surface snow	6.3	0.40 (0.03)	1/38 (1/5)	Yes
27 March 2012	Tundra surface snow	4.9	0.082 (0.009)	1/120 (1/36)	Yes
8 April 2012	Tundra surface snow	4.6	0.24 (0.02)	1/128 (1/14)	Yes
9 April 2012	Tundra surface snow	5.0	0.27 (0.03)	1/60 (1/8)	Yes

Average pH, bromide (Br^-) concentration and bromide/chloride (Br^-/Cl^-) molar ratio are shown for each melted sample with an indication of whether Br_2 was detected for that sample experiment. Standard deviations of multiple analyses are shown in parentheses. Chloride, nitrate, nitrite and sulphate concentrations are shown in Supplementary Table S1. As discussed in the Supplementary Information, the measured snow chemistry is similar to previous observations made across the Arctic region. * indicates that Br_2 was observed only for added $[O_3] > 100$ ppb.

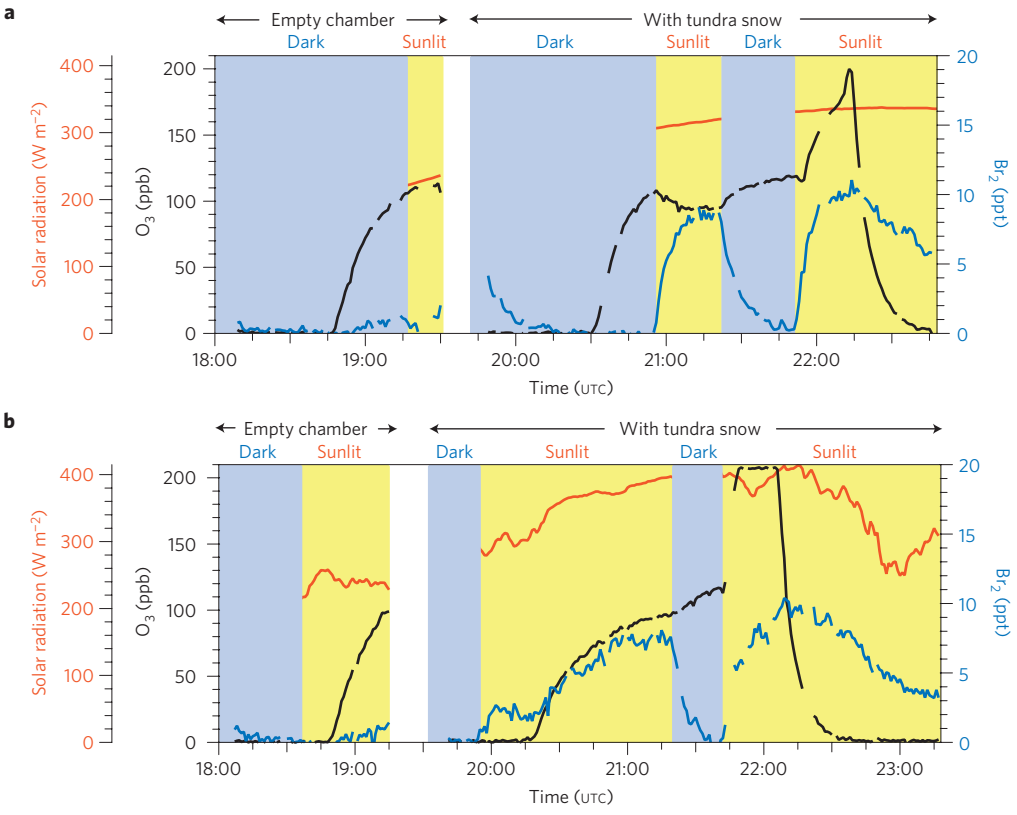

Figure 1 | Br_2 production during snow chamber experiments. a,**b**, Two example tundra surface snow chamber experiments: 27 March 2012 (**a**) and 9 April 2012 (**b**). See Supplementary Information for the other eight experiments with various snow or ice samples. For each experiment, a background test was first conducted using the empty chamber, followed by addition of a snow or ice sample. Br_2 and O_3 concentrations (blue and black lines, respectively) were monitored both in the dark and exposed to solar radiation (orange line), as shown by the light blue and yellow shaded portions of the plots. The Br_2 concentration uncertainty was estimated as 16% + 1 ppt.

sintered snow (8–18 cm above sea ice) collected between these two samples, characterized by a lower pH (5.3) and higher Br^-/Cl^- ratio (1/468), showed Br_2 production only at high O_3 concentrations (>100 ppb) in the sunlight. These trends suggest that frost flowers and brine on the new sea-ice surface, characterized by high pH and low Br^-/Cl^- ratio[15], are not a direct halogen activation source.

Consistent with the snow chamber observations, laboratory studies have shown increased Br_2 production for frozen acidic salt solutions[10,16,17]. This acidity dependence is reflected in the proposed mechanism of initial Br_2 formation, wherein $HO^{\cdot}Br^-$ reacts with H^+ to for $Br^{\cdot}$ within the quasi-brine layer of the snow grains (Fig. 2)[12,17]. A previous study[16] reported higher gaseous HOBr uptake coefficients and reaction probabilities for acidified NaBr/NaCl ice films; however, in similar experiments[18] a pH dependence of Br_2 production from frozen salt surfaces was not observed. Laboratory studies have also shown increased Br_2 production for increasing bromide/chloride ratios of salt

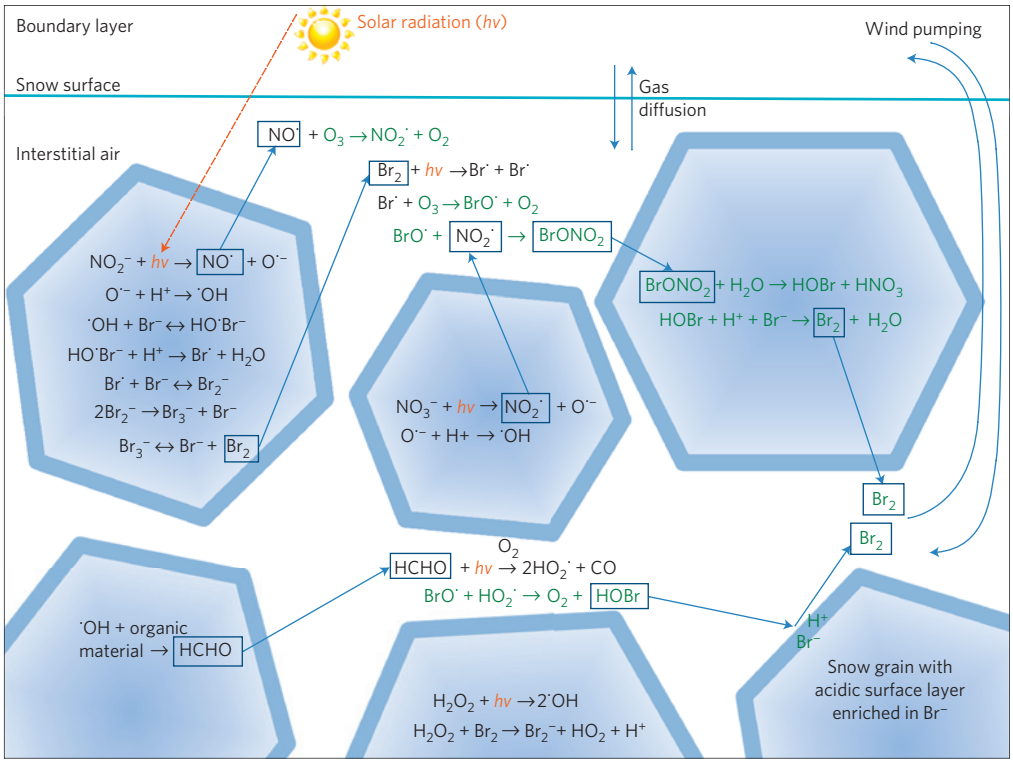

Figure 2 | Snow bromine activation and interstitial air bromine explosion. Proposed major pathways of Br_2 production[10,12,16,17,21] initiated in sunlit, acidified snow, followed by snowpack interstitial air bromine explosion, increasing Br_2 concentrations. Although wind pumping was not active in the chamber, it is an important process for snow exposed to the atmosphere. Reaction pathways requiring O_3 are shown in green. Snow grains do not depict the actual snow morphology. The reactions drawn within the snow grains probably occur in an acidic surface quasi-brine layer[10,13].

solutions and ice films[12,16,18]. Despite the faster reaction of OH with bromide, compared with chloride, the abundance of chloride at lower bromide/chloride ratios results in the dominance of the reaction of OH with chloride[12,18]. This reduces the rate of $HO{\cdot}Br^-$ formation and/or increases the number of steps to Br_2 formation, reducing Br_2 production and resulting in a dependence on the bromide/chloride ratio[12,18]. In our chamber studies, neither BrCl nor Cl_2 was measured above calculated limits of detection (5–8 ppt and 1–6 ppt, respectively, discussed in the Methods). Laboratory studies have shown preferential formation of Br_2 at higher bromide/chloride ratios[18] with $BrCl/Br_2$ being <0.06 (ref. 17), implying BrCl levels that would not have been detectable for this study.

With Br_2 production initialized by snowpack photochemistry, the addition of increasing ozone concentrations to the chamber resulted in increasing Br_2 concentrations, consistent with the autocatalytic bromine explosion mechanism[3,5]. On gas-phase Br_2 photolysis, reaction of bromine atoms ($Br^{\cdot}$) with O_3 forms BrO (Fig. 2). Correspondingly, a decrease in O_3 of ~10% (~10 ppb) was observed when inlet O_3 concentrations were held constant at ~100 ppb and the chamber was exposed to solar radiation (Fig. 1). Subsequent reaction of BrO with gas-phase HO_2 and NO_2 radicals, produced through snowpack photochemistry[19], forms HOBr and $BrONO_2$, respectively (Fig. 2). The snowpack photochemical production of HO_x and NO_x is well known[19], and as expected, nitrogen-containing trace gases were observed when the snow chamber contents were sunlit, as noted in the Supplementary Information. Uptake of HOBr and $BrONO_2$ by the acidic snow surface leads to the formation of more Br_2, which is subsequently released to the gas phase (Fig. 2)[16]. Previous laboratory studies of $BrONO_2$ uptake on HBr-doped ice suggest hydrolysis of $BrONO_2$, forming condensed-phase HOBr, and subsequent reaction with bromide, leading to increased Br_2 release[20,21]. Through this bromine explosion mechanism, the initial condensed-phase formation of one Br_2 molecule leads to the formation of two Br_2 molecules through heterogeneous reactions of HOBr and $BrONO_2$ with the available snowpack Br^- (refs 3,5).

We propose that the bromine explosion pathway occurs most rapidly in the interstitial air of the snowpack with Br_2 release to the atmosphere primarily through wind pumping[7]. As the rate of Br_2 production is dependent on the mass transfer of HOBr (ref. 22) to the snow surface, this process should be more efficient within the snowpack compared with the overlying atmosphere. Consistent with snowpack Br_2 production and interstitial O_3 destruction through the bromine explosion mechanism, Foster *et al.*[23] measured higher bromine and lower O_3 concentrations within the interstitial air of the top 6 cm of the Alert, Canada snowpack, compared with 26 cm above the snow surface. The catalytic bromine cycle also explains our chamber observation of decreased Br_2 concentrations when O_3 was no longer added because BrO, and thus HOBr and $BrONO_2$, could no longer be produced. Further, when the chamber was covered to prevent photochemical reactions, the Br_2 concentrations slowly decayed, as predicted by dilution. It is important to note that Br_2 production was not observed for our snow/ice chamber samples in the dark for concentrations of added O_3 up to 140 ppb; this is in contrast to previous laboratory studies of frozen synthetic sea salt and southern California sea water, which showed Br_2 production following O_3 addition in the dark[24].

During BROMEX, aircraft-based scanner–differential optical absorption spectroscopy[25] (DOAS) measurements were used to examine the spatial variability of BrO, the presence of which reflects local-scale halogen chemistry owing to its short atmospheric

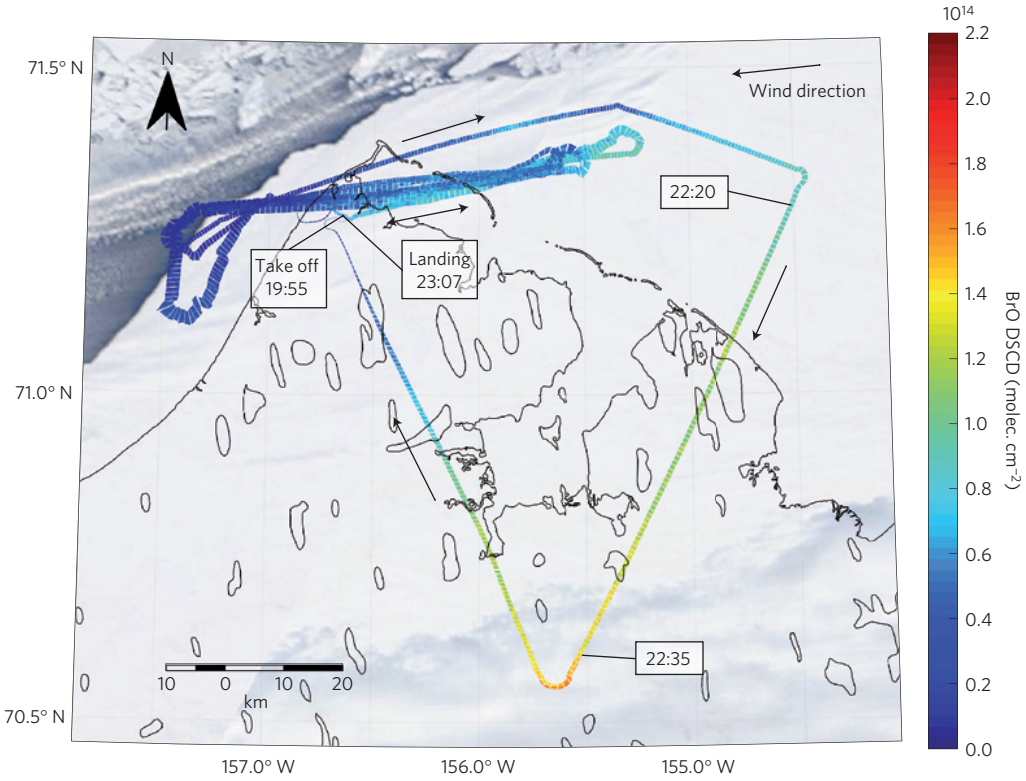

Figure 3 | Spatially resolved BrO. 24 March 2012 aircraft flight track originating from Barrow, Alaska and flying over nearby first-year sea ice, as well inland tundra to the south, at ~900 m above mean sea level (times in UTC). The background snow and sea-ice image is from the MODIS Terra satellite (true colour, 250 m resolution). The black traces correspond to the Alaska coastline and inland snow-covered lakes. Differential slant column densities (DSCDs) of BrO, as measured by the downward-looking scanner–DOAS system, are shown by the colourscale. The retrieved BrO DSCDs have a typical 1σ error of 1.2×10^{13} mol cm^{-2}.

lifetime (typically ~1 min; refs 9,26). During the example flight shown in Fig. 3, BrO was observed over the snow-covered surface of first-year sea ice and tundra. From BrO measurements using a forward-looking DOAS system, discussed in the Supplementary Information and shown in Supplementary Fig. S11, it is concluded that the observed BrO was exclusively located close to the surface. On this day, the highest BrO differential slant column densities were observed over snow-covered tundra, located ~75 km inland; it should be noted that other flights sometimes showed higher BrO concentrations over snow-covered first-year sea ice compared with over tundra. Bromine production and propagation through the snowpack interstitial air bromine explosion mechanism provides an explanation for these observations, which could not be explained by recycling on aerosols, as discussed in the Supplementary Information. It is also consistent with previous satellite-based observations of BrO hotspots above first-year sea ice[7], as well as correlation of BrO concentrations with first-year sea-ice contact[27]. This is because, on average, Arctic first-year sea ice is covered by ~29 cm of snow in the springtime[28], when sunlight can drive the photochemical reactions leading to Br_2 production. A previous study[14] reported brine migration to impact snow only up to ~17 cm above sea ice near Alert (Canada) and Ny-Ålesund (Norway). Therefore, surface snow is most impacted by atmospheric processes, including deposition of sea salt, acidic Arctic haze aerosols, HNO_3 and HOBr (refs 14,29). In addition, the surface snow is more easily acidified than the buffered sea-ice surface[30], making the surface snow more conducive for halogen activation. Similar to surface snow above first-year sea ice, inland tundra snow is also impacted by atmospheric processing and can be characterized by high bromide/chloride ratios due to transport and deposition of gas-phase bromine compounds, as well as sea salt[29].

Snowpack photochemistry leading to interstitial air bromine explosion chemistry and Br_2 release to the atmosphere through wind pumping is an efficient and important mechanism for Arctic halogen activation, leading to ozone and mercury depletion events. The most efficient halogen activation sources were found to be acidic snow (melt water pH < 7) with bromide/chloride ratios greater than ~1/200. The identification of the prominent sources and likely mechanisms of the initiation and propagation of bromine chemistry is expected to improve our ability to simulate atmospheric composition and feedbacks within the Arctic system, particularly with the changing sea-ice landscape. The formation of Br_2 and subsequent destruction of ozone significantly changes the oxidative capacity of the Arctic troposphere, such that the lifetimes of many surface-level trace gas pollutants are significantly reduced[7]. In particular, the reaction of bromine atoms with gaseous elemental mercury, which is transported from the mid-latitudes, leads to toxic mercury deposition to Arctic ecosystems[6]. With climate change, multi-year sea ice is being replaced with first-year sea ice and expanding areas of open ocean[8], changing the precipitation in the Arctic. An increasing fraction of first-year sea ice covered by an acidic snowpack influenced by atmospheric processing will probably lead to more prevalent Br_2 production in the Arctic. The complex interactions and climate system feedbacks between the atmosphere, ocean, sea ice and snowpack influence halogen activation, ozone depletion and mercury deposition to ecosystems in ways that we are just beginning to understand in the changing Arctic system.

Methods

The outdoor snow chamber, shown in Supplementary Fig. S1 and described in the Supplementary Information, was constructed from aluminium with

internal surfaces coated with perfluoroalkoxy to prevent surface reactions. The chamber top consisted of a 0.6-cm-thick sheet of Acrylite OP-4 (CRYO Industries), providing ~60% transmission of 280 nm radiation rising to ~92% at 395 nm; this was covered by opaque fabric for dark experiments. The main chamber (70.5 cm L × 50.0 cm W × 15.0 cm H) provided an internal volume of 53 l. Compressed air (7.4 lpm) of breathing air quality was directed through an activated charcoal hydrocarbon trap to remove volatile organic compounds, followed by a mass flow controller and an O_3 generator (model 97-0067-01, UVP). Experiments consisted of a period with no ozone added, followed by a gradual ramp of the inlet O_3 concentration to ~100 ppb, after which the inlet O_3 concentration was held constant, raised, and then lowered. After passing through the O_3 generator, air was passed through a 3.8 l polyethylene container containing ~1 l of crushed ice produced from milli-Q water to increase the air humidity. Ozone measurements were conducted using a 2B Technologies model 205 dual-beam O_3 monitor.

Ten snow chamber experiments were performed using samples collected near Barrow, Alaska (Table 1). Five tundra snow samples, comprising blocks (~65 cm long × 45 cm wide × 13 cm high) of the top ~13 cm of surface snow, were collected from 8 March to 9 April 2012 at the measurement site ~5 km inland, southeast of the town of Barrow, and placed immediately into the chamber. Other samples were obtained from March 13 to 26, 2012 from a location ~3 km north (upwind) of Barrow on the shore-fast first-year sea ice. These samples included: a block of first-year sea ice, brine icicles collected from below first-year sea ice blocks at a pressure ridge, an 8-cm-thick block of basal snow located directly above the sea ice, a 10-cm-thick block of sintered snow above basal snow, and surface 1 cm of blown and sintered snow. Samples for ion chromatography analysis were stored in sealed polyethylene bags in a −30 °C freezer in Barrow, transported to Indiana packed in dry ice to prevent melting, and then held in a −40 °C freezer until analysis. Melted samples were analysed using a Dionex DX500 ion chromatograph with an AS11 column and suppressed conductivity detection; chloride, bromide, nitrate, nitrite and sulphate concentrations were quantified (Table 1 and Supplementary Table S1). The pH of melted, undiluted samples was measured using a calibrated Thermo Scientific Orion Star Series ISE meter.

Br_2 measurements were conducted using a chemical ionization mass spectrometer, described in ref. 9. Using hydrated I^- ($I^-\cdot(H_2O)_n$) as the reagent ion, Br_2 was measured at masses 287 ($I^{79}Br^{81}Br^-$) and 289 ($I^{81}Br^{81}Br^-$). Background measurements were performed every ~5–15 min during chamber experiments by passing the air flow through a glass wool scrubber. Br_2 in 21 ml min^{-1} N_2 was added to the air flow just before the start of the chamber experiment for calibration; the estimated uncertainty in the reported Br_2 concentrations was 16% + 1 ppt. For chamber periods using O_3-free air, the 3σ limit of detection for Br_2, using mass 287, was calculated to range from ~1–4 ppt (typically ~2 ppt) for a 5 s integration period (corresponding to 1 min of chemical ionization mass spectrometer measurements). Higher 3σ limits of detection (typically ~7 ppt) were calculated for high-[O_3] periods. For all experiments, limits of detection for BrCl (mass 241, $I^{79}Br^{35}Cl^-$, assuming the same sensitivity as mass 287) and Cl_2 (mass 197, $I^{35}Cl^{35}Cl^-$) typically ranged from ~5 to 8 ppt and ~1 to 6 ppt, respectively. Further details are provided in the Supplementary Information.

Airborne BrO measurements were made with a passive DOAS system[25] installed on the Purdue University Airborne Laboratory for Atmospheric Research, a modified Beechcraft Duchess aircraft. The Scanner–DOAS system telescope was mounted below the aircraft. The scanner system was looking downwards (nadir) and featured a whisk broom scanner that pointed the telescope from −25° to +25° (one swath) perpendicular to the flight direction. Each swath had a resolution of 128 pixels and a width about equal to the flight altitude. The telescope received sunlight that was scattered at the ground surface and thus had passed through the atmosphere below the aircraft twice. Spectra were recorded in the range from 300 to 405 nm with a resolution of 0.6 nm. The DOAS data analysis derived BrO differential slant column densities, the total columns of BrO of a light path in comparison with a reference spectrum. Further details are given in the Supplementary Information. In Fig. 3, the data are plotted on a map assigning the BrO differential slant column densities to the ground pixel according to flight position, altitude, pitch and roll.

Received 6 October 2012; accepted 25 February 2013; published online 14 April 2013

References

1. Barrie, L. A., Bottenheim, J. W., Schnell, R. C., Crutzen, P. J. & Rasmussen, R. A. Ozone destruction and photochemical-reactions at polar sunrise in the lower Arctic atmosphere. *Nature* **334,** 138–141 (1988).
2. McConnell, J. C. *et al.* Photochemical bromine production implicated in Arctic boundary-layer ozone depletion. *Nature* **355,** 150–152 (1992).
3. Fan, S-M. & Jacob, D. J. Surface ozone depletion in Arctic spring sustained by bromine reactions on aerosols. *Nature* **359,** 522–524 (1992).
4. Finlayson-Pitts, B. J., Livingston, F. E. & Berko, H. N. Ozone destruction and bromine photochemistry at ground level in the Arctic spring. *Nature* **343,** 622–625 (1990).
5. Vogt, R., Crutzen, P. J. & Sander, R. A mechanism for halogen release from sea-salt aerosol in the remote marine boundary layer. *Nature* **383,** 327–330 (1996).
6. Schroeder, W. H. *et al.* Arctic springtime depletion of mercury. *Nature* **394,** 331–332 (1998).
7. Abbatt, J. P. D. *et al.* Halogen activation via interactions with environmental ice and snow in the polar lower troposphere and other regions. *Atmos. Chem. Phys.* **12,** 6237–6271 (2012).
8. Maslanik, J., Stroeve, J., Fowler, C. & Emery, W. Distribution and trends in Arctic sea ice age through spring 2011. *Geophys. Res. Lett.* **38,** L13502 (2011).
9. Liao, J. *et al.* Observations of inorganic bromine (HOBr, BrO, and Br_2) speciation at Barrow, AK, in spring 2009. *J. Geophys. Res.* **117,** D00R16 (2012).
10. Abbatt, J. *et al.* Release of gas-phase halogens by photolytic generation of OH in frozen halide-nitrate solutions: An active halogen formation mechanism? *J. Phys. Chem. A* **114,** 6527–6533 (2010).
11. France, J. L. *et al.* Hydroxyl radical and NO_x production rates, black carbon concentrations and light-absorbing impurities in snow from field measurements of light penetration and nadir reflectivity of onshore and offshore coastal Alaskan snow. *J. Geophys. Res.* **117,** D00R12 (2012).
12. George, I. J. & Anastasio, C. Release of gaseous bromine from the photolysis of nitrate and hydrogen peroxide in simulated sea-salt solutions. *Atmos. Environ.* **41,** 543–553 (2007).
13. Křepelová, A., Huthwelker, T., Bluhm, H. & Ammann, M. Surface chemical properties of eutectic and frozen NaCl solutions probed by XPS and NEXAFS. *Chem. Phys. Chem.* **11,** 3859–3866 (2010).
14. Domine, F., Sparapani, R., Ianniello, A. & Beine, H. J. The origin of sea salt in snow on Arctic sea ice and in coastal regions. *Atmos. Chem. Phys.* **4,** 2259–2271 (2004).
15. Douglas, T. A. *et al.* Frost flowers growing in the Arctic ocean–atmosphere–sea ice-snow interface: 1. Chemical composition. *J. Geophys. Res.* **117,** D00R09 (2012).
16. Huff, A. K. & Abbatt, J. P. D. Kinetics and product yields in the heterogeneous reactions of HOBr with ice surfaces containing NaBr and NaCl. *J. Phys. Chem. A* **106,** 5279–5287 (2002).
17. Sjostedt, S. J. & Abbatt, J. P. D. Release of gas-phase halogens from sodium halide substrates: Heterogeneous oxidation of frozen solutions and desiccated salts by hydroxyl radicals. *Environ. Res. Lett.* **3,** 045007 (2008).
18. Adams, J. W., Holmes, N. S. & Crowley, J. N. Uptake and reaction of HOBr on frozen and dry NaCl/NaBr surfaces between 253 and 233 K. *Atmos. Chem. Phys.* **2,** 79–91 (2002).
19. Dominé, F. & Shepson, P. B. Air–snow interactions and atmospheric chemistry. *Science* **297,** 1506–1510 (2002).
20. Sumner, A. L. & Shepson, P. B. Snowpack production of formaldehyde and its effect on the Arctic troposphere. *Nature* **398,** 230–233 (1999).
21. Aguzzi, A. & Rossi, M. J. Heterogeneous hydrolysis and reaction of $BrONO_2$ and Br_2O on pure ice and ice doped with HBr. *J. Phys. Chem. A* **106,** 5891–5901 (2002).
22. Nissenson, P., Packwood, D. M., Hunt, S. W., Finlayson-Pitts, B. J. & Dabdub, D. Probing the sensitivity of gaseous Br_2 production from the oxidation of aqueous bromide-containing aerosols and atmospheric implications. *Atmos. Environ.* **43,** 3951–3962 (2009).
23. Foster, K. L. *et al.* The role of Br_2 and BrCl in surface ozone destruction at polar sunrise. *Science* **291,** 471–474 (2001).
24. Oum, K. W., Lakin, M. J. & Finlayson-Pitts, B. J. Bromine activation in the troposphere by the dark reaction of O_3 with seawater ice. *Geophys. Res. Lett.* **25,** 3923–3926 (1998).
25. Platt, U. & Stutz, J. *Differential Optical Absorption Spectroscopy: Principles and Applications, Physics of Earth and Space Environments* (Springer, 2008).
26. Langendorfer, U., Lehrer, E., Wagenbach, D. & Platt, U. Observation of filterable bromine variabilities during Arctic tropospheric ozone depletion events in high (1 hour) time resolution. *J. Atmos. Chem.* **34,** 39–54 (1999).
27. Simpson, W. R. *et al.* First-year sea-ice contact predicts bromine monoxide (BrO) levels at Barrow, Alaska better than potential frost flower contact. *Atmos. Chem. Phys.* **7,** 621–627 (2007).
28. Kwok, R. *et al.* Airborne surveys of snow depth over Arctic sea ice. *J. Geophys. Res.* **116,** http://dx.doi.org/10.1029/2011JC007371 (2011).
29. Krnavek, L. *et al.* The chemical composition of surface snow in the Arctic: Examining marine, terrestrial, and atmospheric influences. *Atmos. Environ.* **50,** 349–359 (2012).
30. Wren, S. N. & Donaldson, D. J. How does deposition of gas phase species affect pH at frozen salty interfaces? *Atmos. Chem. Phys.* **12,** 10065–10073 (2012).

Acknowledgements

Financial support was provided by the National Science Foundation Office of Polar Programs (ARC-1107695) and the National Aeronautics and Space Administration (NASA) Cryospheric Sciences Program as a part of the NASA Interdisciplinary Research on Arctic Sea Ice and Tropospheric Chemical Change (09-IDS09-31). K.A.P. is supported by a National Science Foundation Postdoctoral Fellowship in Polar Regions Research. S. V. Nghiem is thanked for BROMEX organization. The MODIS image in Fig. 3 was provided by the NASA Rapid Response MODIS Subset in support of BROMEX. R. Replogle (Purdue University) is thanked for construction of the snow chamber. Solar radiation data were acquired by and obtained from the NOAA/ESRL/GMD Solar Radiation group. We are grateful to UMIAQ and CH2M Hill Polar Services for field logistical assistance. M. O. L. Cambaliza and D. Caulton (Purdue University) are thanked for aircraft attitude data used in the DOAS analysis. E. Boone (Purdue University) is thanked for aerosol data analysis. M. Sturm (CRREL) is thanked for chamber design advice. J. W. Halfacre (Purdue University) is thanked for calibration of the ozone monitor. R. Lieb-Lappen (Dartmouth University) is thanked for field discussions. This is publication 1241 of the Purdue Climate Change Research Center.

Author contributions

P.B.S. and K.A.P. designed the experiments, which were conducted by K.A.P. and K.D.C. K.A.P. wrote the manuscript. P.B.S., K.A.P, K.D.C. and M.C. designed the snow chamber. T.A.D. collected samples from the sea ice, provided guidance for tundra snow sampling and contributed to discussions. P.B.S., D.P., S.G. and J.Z. conducted the aircraft-based BrO measurements with aircraft assistance from B.H.S. W.R.S. and U.P. contributed to discussions and were other principal investigators of the BrO study. D.J.T. and L.G.H. provided assistance with chemical ionization mass spectrometry. All authors reviewed and commented on the paper.

Additional information

Supplementary information is available in the online version of the paper. Reprints and permissions information is available online at www.nature.com/reprints. Correspondence and requests for materials should be addressed to K.A.P.

Competing financial interests

The authors declare no competing financial interests.